A New Approach to Interfacial Energy. 3. Formulation of the Absolute Value of the Solid−Liquid Interfacial Energy and Experimental Collation to Silver Halide Systems†

Tadao Sugimoto* and Fumiyuki Shiba

Institute for Advanced Materials Processing, Tohoku University, Katahira 2-1-1, Aobaku, Sendai 980-8577, Japan

Received: November 9, 1998; In Final Form: March 2, 1999

A new theoretical formula for the absolute value of the interfacial energy of the solid−liquid interface has been derived on the basis of the fundamental theory of interfacial energy described in *J. Colloid Interface Sci.* **1996**, *181*, 259; **1996**, *183*, 299. Namely, the intrinsic specific interfacial energy of a solid−liquid interface without adsorption is given by $\gamma = -N^{\sigma}\lambda kT \ln x_{(\infty)}$, where N^{σ} is the surface density of the surface monomers of the solid, λ is the ratio of the number of open bonding sites of a surface monomer to that of a free monomer, k is the Boltzmann constant, T is the absolute temperature, and $x_{(\infty)}$ is the solubility of the bulk solid in terms of mole fraction of the monomers in the liquid phase against the total mole numbers of the solution components including the solvent molecules. Here, "monomer" refers to the minimum subunit of the solid such as AgCl, AgBr, etc. The formula has been collated to the experimental results of γ for AgCl, AgBr, and AgI, determined by potentiometric measurement of the size-dependent solubilities of these silver halide particles with the Gibbs−Thomson equation. The experimental results were in excellent agreement with the theoretical values for the silver halides. Also, some fundamental problems were found to be involved in Tolman's theory for size dependence of γ, and it has been deduced that γ must be independent of particle size, as has been confirmed by experiment.

1. Introduction

Interfacial energy of the solid−liquid interface is one of the most fundamental determinants for nucleation and growth of colloidal particles, modification of crystal habits, adsorption phenomena to solid surfaces, etc. Unfortunately, however, we have no direct method to measure the interfacial energies of solid−liquid and solid−gas interfaces, in contrast to liquid−gas and liquid−liquid interfaces. Hence, presently available data for solid−liquid interfaces have been obtained indirectly from turbidimetry during nucleation of precipitates on the basis of the classical nucleation theories,[1−7] solubility measurement with the Gibbs−Thomson equation,[8−10] etc. However, they are mostly unsatisfactory in reliability, since the widely scattered results obtained from the classical nucleation theories, based on a multitude of assumptions and approximations, are not suitable for the precise evaluation of the interfacial energy and since systematic measurement of γ using the Gibbs−Thomson effect has never been performed. In addition, the understanding of essential nature of the interfacial energy itself seems to be far from satisfactory.

In view of this situation, Sugimoto[11] proposed a new theoretical approach to the interfacial energy and derived a fundamental equation in part 1 of this series (eq 2.16 in ref 11). In part 2,[12] the fundamental theory has been applied to the formulation of the interfacial energies of different interfaces changing with adsorption. However, the benefit of the fundamental theory is not limited only to the full description of the individual behavior of interfacial molecules, but also it will enable us to formulate the absolute value of the interfacial energy, as different from Gibbs' theory on the interfacial energy. The objectives of the study of this part 3 are to derive the formula for the absolute value of the solid−liquid interfacial energy of pure spherical and polyhedral particles on the basis of the fundamental theory, and its experimental verification by systematic potentiometry on the size-dependent solubilities of silver halide sols such as AgCl, AgBr, and AgI on the basis of the Gibbs−Thomson effect. Finally, in the Discussion, we will discuss the significance of the present theory in comparison with the existing theories, the shape effect on γ, the effective particle radius for overall solubility, and Tolman's theory[13] for the size dependence of γ.

2. Formulation of Solid−Liquid Interfacial Energy

2.1. Interfacial Energy of Spherical Particles. First of all, we define a term "monomer" as the minimum subunit of a solid, equivalent to a neutral molecule of the solid, e.g., AgCl, TiO_2, Fe_2O_3, etc. A monomer in a liquid phase means a dissolved neutral molecule, and thus, it is distinguished from other complexes or dissociated ions. Similarly, "*n*-mer" can be defined as a particle composed of *n* monomers.

When a monomer in a pure solid phase α, X^{α}, transfers to an adjacent liquid phase β through the scission of the surrounding bondings of the solid, the liberated monomer X may be immediately solvated by the solvent molecules, L, as

$$X^{\alpha} + mL \rightarrow XL_m \tag{2.1}$$

where m is the number of solvent molecules coordinated to a monomer X. In this process, the free energy of formation of XL_m per one molecule, ψ^0, is given by

* To whom correspondence should be addressed.

† Presented in part at the 50th Symposium on Colloid and Interface Chemistry, Saga, October 8−10, 1997.

10.1021/jp984348g CCC: $18.00
Published on Web 04/16/1999

$$\psi^0 = \mu^{\Theta}_{XL_m} - \mu^{0,\alpha}_X - m\mu^*_L \quad (2.2)$$

where $\mu^{\Theta}_{XL_m}$ is the standard chemical potential of one XL_m molecule, $\mu^{0,\alpha}_X$ is that of X in solid phase α, and μ^*_L is the chemical potential of L in the liquid phase β which contains XL_m therein. The superscript Θ of $\mu^{\Theta}_{XL_m}$ indicates μ_{XL_m} at the mole fraction $x_{XL_m} = 1$ obtained by extrapolation from $x_{XL_m} \ll 1$, while the superscript 0 of $\mu^{0,\alpha}_X$ means the chemical potential of X in the pure solid phase α ($x^\alpha_X = 1$). In a diluted solution of XL_m, μ^*_L is a constant given by $\mu^*_L = \mu^0_L + kT \ln(1 - x_{XL_m})$, where x_{XL_m} is the mole fraction of XL_m at equilibrium with the bulk solid ($=x_{(\infty)}$ in eq 2.3). As $(1 - x_{XL_m})$ is usually very close to unity for a sparingly soluble solid which we deal with, μ^*_L can be regarded equal to μ^0_L in most cases. The ψ^0 corresponds to the interfacial energy of a monomer X in liquid phase β (see ref 11, Section 2).

If the system is in equilibrium, there is the following relation among the chemical potentials of X in the α phase ($\mu^{0,\alpha}_X$), XL_m in the β phase (μ_{XL_m}), and L in the β phase (μ^*_L) from eq 2.1:

$$\mu^{0,\alpha}_X + m\mu^*_L = \mu_{XL_m} = \mu^{\Theta}_{XL_m} + kT \ln x_{(\infty)} \quad (2.3)$$

where $x_{(\infty)}$ is the mole fraction of X in the form of XL_m in the β phase in equilibrium with the bulk solid of radius $r = \infty$. Hence, it follows from eqs 2.2 and 2.3 that

$$\psi^0 = -kT \ln x_{(\infty)} \quad (2.4)$$

As the solid is assumed to be a sparingly soluble species, $x_{(\infty)}$ is sufficiently small to be given by

$$x_{(\infty)} = c_{(\infty)}\upsilon_0 \quad (2.5)$$

where $c_{(\infty)}$ is the solubility of bulk solid in the number concentration of the monomers and υ_0 is the molecular volume of the solvent.

As a rule, an amorphous *n*-mer particle composed of a large number of randomly oriented *n* monomers is of a spherical shape. In this case, if the monomers are also originally spherical but sufficiently soft to adjust their shape to be densely packed without pores in a *n*-mer, the surface area of the *n*-mer, a_n, is rigorously given by

$$a_n = a_1 n^{2/3} = (36\pi\upsilon_1^2)^{1/3} n^{2/3} \quad (2.6)$$

where a_1 and υ_1 are the surface area and the volume of an unsolvated monomer, respectively. Therefore, the interfacial energy of *n*-mer, ψ^0_n, is given by

$$\psi^0_n = \psi^0 n^{2/3} \quad (2.7)$$

The intrinsic specific interfacial energy or the interfacial energy per unit area in the absence of adsorption, γ^0, for spherical *n*-mer particles is given by

$$\gamma^0 = \frac{\psi^0_n}{a_n} = \frac{\psi^0}{a_1} = \frac{-kT \ln x_{(\infty)}}{(36\pi\upsilon_1^2)^{1/3}} \quad (2.8)$$

where γ^0 specifically denotes γ without adsorption.

This equation has been derived on the assumption that the monomer is spherical. However, if we consider that each monomer has a definite number of discrete sites for bonding with additional monomers or for coordination of solvent molecules, as will be discussed in detail in the next section, these active sites correspond to discrete sources of the interfacial energy, so that γ^0 is determined only by the number and each activity of the bonding sites of a monomer, regardless of its shape. In this case, the interfacial energy of a monomer, γ^0, is equal to that of a spherical monomer with the same volume and the same number of active sites. Thus, the interfacial energy per unit area of a spherical particle composed of the randomly oriented monomers may be regarded as equal to the specific interfacial energy of the equivalent spherical monomer. In other words, eq 2.8 for spherical particles may hold regardless of the original shape of the monomers.

Polycrystal particles consisting of randomly oriented subcrystals are also normally spherical, and it is not rare to find that even single-crystal particles become spherical in the early stage of growth to minimize their specific surface area or in the course of dissolution. The interfacial energies of these particles may also be given by eq 2.8.

2.2. Interfacial Energy of Polyhedral Particles. Polyhedral particles are usually of a monocrystalline structure having a specific orientation of solid monomers at surfaces. In this case, the geometry of the crystal surfaces must be taken into account for the derivation of their interfacial energies.

Here, we introduce a concept of "open bonding sites" or simply "open sites" as neutral discrete centers of the interfacial energy of a monomer. Common monomers of crystals consist of more than two kinds of atoms, such as AgBr, TiO_2, Fe_2O_3, etc. For example, a AgBr monomer in the rock salt crystal consists of a Ag atom and a Br atom with the same coordination number, 6. In other words, a Ag atom and a Br atom in a AgBr monomer have six positive bonding spots and six negative bonding spots, respectively. Since a positive bonding spot of a Ag atom and a negative bonding spot of a Br atom have been used to form a AgBr monomer, the remaining numbers of positive and negative free bonding spots of a AgBr monomer are both 5. A pair of a positive and a negative free bonding spot constitutes one open site. In the absence of adsorption, there are equal numbers of positive and negative free bonding spots to form the same number of open sites on a surface monomer of any kind of crystal structures.

As obvious from the definition of the open site, it is a site for bonding of an additional neutral monomer. The reason for considering such an open site is that even ionic crystals are eventually grown or dissolved through a monomer unit to keep the internal neutrality of the solid and a constant surface charge even if the surfaces are electrically charged. Thus, this concept can commonly be applied to nonionic solids as well.

The interfacial energy per one surface monomer, $\psi^{0,\sigma}$, is defined as

$$\psi^{0,\sigma} = \mu^{0,\sigma}_{XL_{m'}} - \mu^{0,\alpha}_X - m'\mu^*_L \quad (2.9)$$

where $\mu^{0,\sigma}_{XL_{m'}}$ is the standard chemical potential of a surface monomer coordinated by m' solvent molecules, m' is the number of solvent molecules L coordinated to a monomer X in the surface layer of the solid phase. The interfacial energy per open site, ϵ, can be written as

$$\epsilon = \frac{\psi^{0,\sigma}}{n^\sigma_s} = \frac{\psi^0}{n_s} \quad (2.10)$$

where n^σ_s and n_s are the numbers of the open sites for a monomer in the surface layer of the solid phase and for a free monomer in the liquid phase, respectively. From eqs 2.4 and 2.10, $\psi^{0,\sigma}$ can be represented by

$$\psi^{0,\sigma} = \frac{n_s^\sigma}{n_s}\psi^0 = -\frac{n_s^\sigma}{n_s} kT \ln x_{(\infty)} \tag{2.11}$$

Thus, the specific interfacial energy of the solid−liquid interface without adsorption, γ^0, is represented by

$$\gamma^0 = N^\sigma \psi^{0,\sigma} = N^\sigma \lambda \psi^0 = -N^\sigma \lambda kT \ln x_{(\infty)} \tag{2.12}$$

where N^σ is the surface density of monomers at the solid surface and $\lambda \equiv n_s^\sigma/n_s$ ($=m'/m$). In the case of a sphere, $N^\sigma\lambda = (36\pi v_1^2)^{-1/3}$ from eq 2.8.

Equation 2.12 can be derived directly from the fundamental equation 2.16 in ref 11 as well. Namely, i and j in eq 2.16 in ref 11 correspond to X and L, respectively, so that

$$\begin{aligned}
\gamma^0 &= N_i^\sigma(\mu_i^{\sigma_A} - \mu_i^\alpha) + N_j^\sigma(\mu_j^{\sigma_B} - \mu_j^\beta) \\
&= N^\sigma[(\mu_X^{0,\sigma_A} - \mu_X^{0,\alpha}) + m'(\mu_L^{0,\sigma_B} - \mu_L^*)] \\
&= N^\sigma(\mu_{XL_{m'}}^{0,\sigma} - \mu_X^{0,\alpha} - m'\mu_L^*) \\
&= N^\sigma\left[\frac{m'}{m}\mu_{XL_m}^\Theta + \left(1 - \frac{m'}{m}\right)\mu_X^{0,\alpha} - \mu_X^{0,\alpha} - m'\mu_L^*\right] \\
&= N^\sigma\lambda(\mu_{XL_m}^\Theta - \mu_X^{0,\alpha} - m\mu_L^*) \\
&= N^\sigma\lambda\psi^0
\end{aligned}$$

If we define the standard chemical potential of a surface monomer, $\mu_X^{0,\sigma}$, as

$$\mu_X^{0,\sigma} \equiv \mu_{XL_{m'}}^{0,\sigma} - m'\mu_L^* \tag{2.13}$$

γ^0 may be simply written as

$$\gamma^0 = N^\sigma(\mu_X^{0,\sigma} - \mu_X^{0,\alpha}) \tag{2.14}$$

Furthermore, if we define the standard chemical potential of a monomer in the liquid phase, μ_X^Θ, in a similar manner as

$$\mu_X^\Theta \equiv \mu_{XL_m}^\Theta - m\mu_L^* \tag{2.15}$$

ψ^0 is given by

$$\psi^0 = \mu_X^\Theta - \mu_X^{0,\alpha} \tag{2.16}$$

Hence, the chemical potential of X at mole fraction x in the liquid phase, μ_X, is written by

$$\mu_X = \mu_X^\Theta + kT \ln x \tag{2.17}$$

At equilibrium with the bulk solid phase α, it follows from eq 2.3 that

$$\mu_X = \mu_X^{0,\alpha} \tag{2.18}$$

where $x = x_{(\infty)}$. The chemical potential of X in the form of μ_X in eq 2.17 can be used regardless of the degree of solvation of X, so it may be more convenient than the form of μ_{XL_m} when a simple equilibrium between pure solid and its solution is considered.

3. Theoretical Calculation of Interfacial Energies of Silver Halides

For the test of the theory of solid−liquid interfacial energy, we have chosen silver halide microcrystals because of their practical importance as photographic materials and the repletion with precise experimental data on the complex chemistry.[14,15]

Fundamental parameters of structural and thermodynamic properties of silver halides of interest, necessary for the theoretical calculation of γ^0, are summarized in Table 1. Since AgI is normally precipitated as a mixture of β-AgI (wurtzite-type; hexagonal) and γ-AgI (zinc-blend-type; cubic) around room temperature, the used characteristic parameters from v_1 to $x_{(\infty)}$ in Table 1 are those of the mixture.

As the coordination numbers of cation and anion of AgCl or AgBr are 6, the number of the total open sites of a AgX monomer (hereafter X denotes the arbitrary halide, and not a monomer), n_s, is 5, whereas the coordination number of cation or anion of AgI of both types is 4, corresponding to n_s equal to 3.

The molecular volumes, v_1, for AgCl and AgBr were obtained from their lattice parameters. For v_1 of AgI, we used 6.88×10^{-23} cm^3 calculated from the overall specific gravity (=5.67).[16] The molar volume was obtained from v_1 multiplied by the Avogadro number.

The mole fraction of AgX monomers in water can be obained from eq 2.5 ($x_{(\infty)} = c_{(\infty)}v_0 = C_{(\infty)}V_0$) with their molar concentration, $C_{(\infty)}$, and the molar volume of water, V_0 ($=1.81 \times 10^{-2}$ dm^3 mol^{-1} at 25 °C). Here, $C_{(\infty)}$ is given as a product of the solubility product (K_{sp}) and the stability constant of AgX monomers (β_{11}); i.e.,

$$C_{(\infty)} = K_{sp}\beta_{11} \tag{3.1}$$

where $K_{sp} = [Ag^+][X^-]$ and $\beta_{11} = [AgX]/([Ag^+][X^-])$. The thermodynamic parameters, K_{sp} and β_{11}, are available in the literature.[14,15] For AgCl and AgBr (fcc crystals), the surface densities of monomers, N^σ, are given by $2/a_0^2$, $\sqrt{2}/a_0^2$, and $2/\sqrt{3}a_0^2$ for {100}, {110}, and {111} faces, respectively, where a_0 is the lattice parameter. The molecular volume v_1 is given by $a_0^3/4$. For β-AgI, N^σ of the {0001} and {10$\bar{1}$0} faces are given by $1/\sqrt{3}a_0^2$ and $1/a_0c_0$, respectively, whereas those of the {100}, {110}, and {111} faces for γ-AgI are given by $1/a_0^2$, $\sqrt{2}/a_0^2$, and $2/\sqrt{3}a_0^2$, respectively. On the other hand, the number of the open sites of a surface monomer n_s^σ also depends on the surface structure.

In the determination of N^σ and n_s^σ of the {111} face of fcc crystals including AgCl and AgBr, it seems convenient to postulate an octahedral particle bound by eight {111} regular faces, in which four of them are covered with only Ag atoms and the other four with only halide (X) atoms alternately. In this model, an X plane is located at the reverse side of a Ag plane. Thus, it can be interpreted that one Ag atom in a surface layer and one X atom in the reverse side surface layer constitute one AgX monomer. However, if there is no adsorption of ions, actual {111} surfaces of an octahedral particle are supposed to be neutral by randomly distributing ions of the opposite charge through occupying about half of the open spots of the regular surfaces to minimize the total surface energy. Even so, the surface monomer density N^σ and the number of open sites of a surface monomer, n_s^σ, must be the same, because the total number of open sites of a particle is unchanged by this process.

The parameters, N^σ, n_s^σ, and λ proper to the individual face indices are summarized in Table 2. The theoretical γ^0 values for different silver halide particles with various facets are calculated from eqs 2.8 and 2.12 with these parameters and shown in the last column of Table 2.

TABLE 1: Fundamental Parameters of Structural and Thermodynamic Properties for Silver Halides (25 °C)[a]

silver halides	AgCl	AgBr	AgI	
			β	γ
structure	fcc rock salt	fcc rock salt	hexagonal wurzite	fcc zinc-blende
lattice parameter (Å)	5.5502	5.7748	$a = 4.59$ $c = 7.52$	6.48
coordination number of an atom	6	6	4	4
open sites of a free monomer, n_s	5	5	3	3
molecular volume, v_1 (cm^3)	4.27×10^{-23}	4.81×10^{-23}	6.88×10^{-23}	
molar volume, V_m ($cm^3\ mol^{-1}$)	25.9	29.0	41.4	
solubility product, K_{sp} ($mol^2\ dm^{-6}$)	1.79×10^{-10}	4.90×10^{-13}	8.32×10^{-17}	
stability constant, β_{11} ($dm^3\ mol^{-1}$)	2.0×10^3	3.2×10^4	3.2×10^7	
monomer solubility, $c_{(\infty)}$ (dm^{-3})	2.13×10^{17}	9.27×10^{15}	1.60×10^{15}	
monomer solubility, $C_{(\infty)}$ ($mol\ dm^{-3}$)	3.53×10^{-7}	1.54×10^{-8}	2.65×10^{-9}	
monomer solubility, $x_{(\infty)}$	6.39×10^{-9}	2.79×10^{-10}	4.80×10^{-11}	

[a] The parameters from v_1 to $x_{(\infty)}$ for AgI are those of the overall values for a mixed precipitates of β- and γ-AgI. v_1 values for AgCl and AgBr were calculated from the respective lattice parameters. Different notations for monomer solubility, $c_{(\infty)}$, $C_{(\infty)}$, and $x_{(\infty)}$, designate number concentration, molarity, and mole fraction, respectively.

TABLE 2: Parameters Used in the Theoretical Calculation of the Interfacial Energies and the Results of the Calculations at 25 °C[a]

	AgCl				AgBr				AgI[b]	β-AgI		γ-AgI		
	sphere	{100}	{110}	{111}	sphere	{100}	{110}	{111}	sphere	{0001}	{1010}	{100}	{110}	{111}
N^σ (nm^{-2})		6.493	4.591	3.748		5.997	4.241	3.463		2.740	2.897	2.390	3.373	2.754
n_s^σ		1	2	3		1	2	3		1	2	2	1	2
$\lambda(=n_s^\sigma/n_s)$		1/5	2/5	3/5		1/5	2/5	3/5		1/3	2/3	2/3	1/3	2/3
γ^0 ($mJ\ m^{-2}$)	131	101	143	175	142	109	154	188	121	89.4	189	156	110	180

[a] $N^\sigma_{100}/N^\sigma_{110}/N^\sigma_{111} = 1:1/\sqrt{2}:1/\sqrt{3}$; $\gamma^0_{100}/\gamma^0_{110}/\gamma^0_{111} = 1:1/\sqrt{2}:1/\sqrt{3}$ for AgCl and AgBr. [b] AgI = mixed precipitate of β- and γ-AgI.

4. Experimental

4.1. Determination of Interfacial Energy by Gibbs−Thomson Effect. The increase of solubility with decreasing particle size is a well known phenomenon as the Gibbs−Thomson effect, as described by the following simple formula:

$$C_{(r)} = C_{(\infty)} \exp\left(\frac{2V_m\gamma}{rRT}\right) \tag{4.1}$$

where $C_{(r)}$ and $C_{(\infty)}$ are the concentrations of monomers in equilibrium with a particle of radius r and a bulk solid of $r = \infty$, respectively. The equation can readily be derived from the maximum free energy necessary for the formation of a particle of finite dimensions with a specific interfacial energy γ from a supersaturated solution. For this derivation, apart from the presence of γ, any knowledge on the background of γ is not required. On the other hand, the explicit formulas for γ^0 in eqs 2.8 and 2.12 have been derived from the insight into the origin of γ. As a consequence, the backgrounds of the Gibbs−Thomson equation in eq 4.1 and the formulas for γ^0 in eqs 2.8 and 2.12 are essentially different so that the experimental results of γ^0 on the basis of the Gibbs−Thomson effect may be used as a test of the present theory of γ^0. Because of the simple and thermodynamically correct formula, the Gibbs−Thomson equation is expected to prove its usefulness in obtaining reliable data of γ^0, if we use the well established potentiometric technique with a Ag/Ag_2S electrode in silver halide systems.

As obvious from eqs 3.1 and 4.1, the Gibbs−Thomson equation for a dissociative material is also written as

$$K^r_{sp} = K^\infty_{sp} \exp\left(\frac{2V_m\gamma}{rRT}\right) \tag{4.2}$$

where K^r_{sp} and K^∞_{sp} are the solubility products of particles of radius r and ∞, respectively. When either cation or anion is in a large excess, the supersaturation ratio, S_r, is determined by the concentration ratio of the minor ions. For example, if $[X^-] \gg \sqrt{K_{sp}}$,

$$S_r \equiv \frac{C_{(r)}}{C_{(\infty)}} = \frac{K^r_{sp}}{K^\infty_{sp}} = \frac{[Ag^+]}{[Ag^+]_\infty} = \exp\left(\frac{2V_m\gamma}{rRT}\right) \tag{4.3}$$

where $[Ag^+]_r$ and $[Ag^+]_\infty$ are the concentrations of silver ions in equilibrium with AgX particles of radius r and ∞, respectively. Therefore, if the particle sizes and corresponding solubility ratios, S_r, are experimentally measured, the interfacial energy will be determined from the slope of the linear line passing through the origin for the plot of $\ln S_r$ vs r^{-1},

$$\ln S_r = \frac{2V_m\gamma}{RT}\frac{1}{r} \tag{4.4}$$

Incidentally, though this equation is for spherical particles, the corresponding equation for regular polyhedral particles having a inscribed sphere of radius r can be represented by the same formula as eq 4.3, as shown in the Appendix.

4.2. Experimental Conditions. An amount of 10 cm^3 of 1.10×10^{-3} mol dm^{-3} $AgNO_3$ solution was added to 100 cm^3 of a well stirred potassium halide solution of a certain concentration at a constant temperature in a water bath to precipitate silver halide particles (1.0×10^{-4} mol dm^{-3}). The concentrations of the used KCl, KBr, and KI solutions were 1.21×10^{-3}, 2.20×10^{-4}, and 1.21×10^{-4} mol dm^{-3}, respectively, to make the respective pX values as pCl = 3.0, pBr = 4.0, and pI = 5.0 after mixing, where the definition of pX is as follow:

$$pX \equiv -\log[X^-] \tag{4.5}$$

These pX conditions give almost the minimum solubilities, as the total of all kinds of halide complexes, for the respective

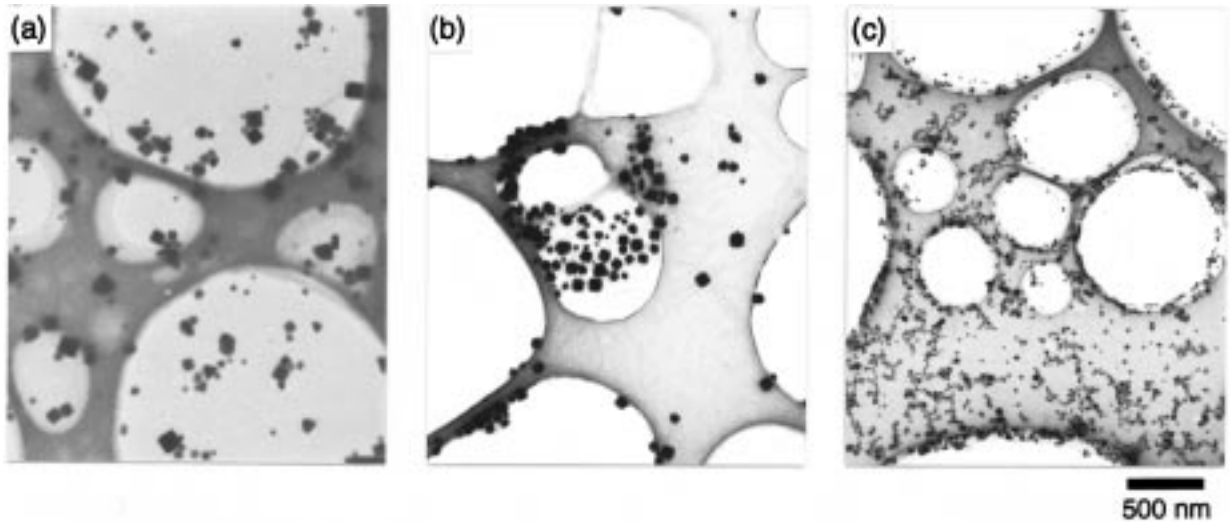

Figure 1. TEM micrographs of silver halide particles prepared under standard conditions of each system at 25 °C and sampled ca. 100 min after the addition of $AgNO_3$: (a) AgCl; (b) AgBr; (c) AgI.

silver halides around room temperature.[14,15] The temperature was varied as 10, 20, 25, 30, and 40 °C in this study.

The equilibrium concentration of Ag^+ for each particle radius was automatically measured with a Ag/Ag_2S on a Ag plate (previously cleaned with ammonia, nitric acid, and distilled water) in a 0.01 mol dm^{-3} Na_2S solution at a constant current (∼5 mA) for ca. 10 min. Calibration lines for silver potential versus pX in a suspension of sufficiently large AgX crystals saturated with silver ions were in excellent conformity with the Nernst equation. From this measurement, $C_{(\infty)}$ values were also determined. A Ag/AgCl electrode in 0.10 mol dm^{-3} KCl with sufficiently large AgCl particles was employed as a reference connected to sample sols through a salt bridge containing 2 mol dm^{-3} KNO_3 and 1.5% agar.

The mean particle size was determined from the size analysis based on transmission electron micrographs (TEM). The arithmetic mean of the radii of ca. 300 particles was used as the mean radius. To make TEM specimens, each silver halide sol taken on a TEM microgrid was instantly frozen in liquid nitrogen to quench the particle growth, followed by freeze-drying without melting.

5. Results

Typical TEM micrographs of AgCl, AgBr, and AgI particles obtained in experiments at 25 °C are shown in Figure 1. The particles were found to be cubic for AgCl, nearly cubic for AgBr, and spherical for AgI.

Typical time evolutions of the supersaturation ratio $S_r(=C_{(r)}/C_{(\infty)})$ and the mean particle radius ($=d/2$; d = the mean edge length for cubic particles) in a AgCl system at 25 °C and pCl = 3.0 are shown in Figure 2. Figure 3 shows the relationship between the mean particle size and the supersaturation ratio with data of repeated runs for the AgCl system at 25 °C and pCl = 3.0.

Figure 4 shows all correlations between $\ln S_r$ and r^{-1} for AgCl, AgBr, and AgI systems. Obviously, a linear relationship passing through the origin is observed for all cases. From the slopes of the straight lines in Figure 4 and V_m values in Table 1, the experimental γ^0 values were determined as a function of temperature in the range 10−40 °C, as shown in Table 3.

On the other hand, for calculation of theoretical γ^0 at different temperatures, we used K_{sp} and β_{11} as functions of temperature.

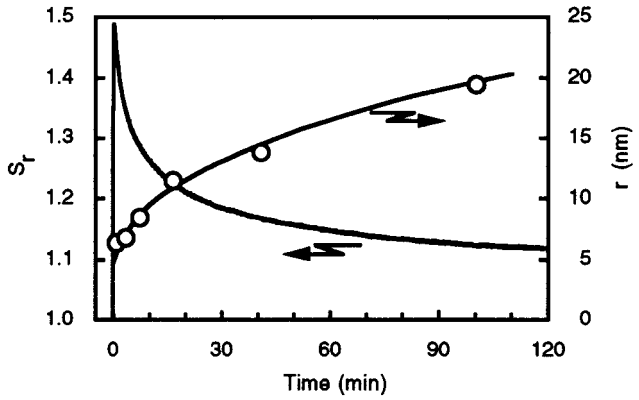

Figure 2. Typical time evolutions of supersaturation ratio and average radius of AgCl particles at 25 °C and pCl = 3.0.

Fortunately, pK_{sp} ($\equiv -\log K_{sp}$) for each silver halide is given as a function of temperature in centigrade, t, as

$$pK_{sp}^{AgCl} = 10.830 - 4.79 \times 10^{-2}\, t + 2.03 \times 10^{-4} t^2 - 4.33 \times 10^{-7} t^3$$

$$pK_{sp}^{AgBr} = 13.702 - 6.17 \times 10^{-2} t + 2.57 \times 10^{-4} t^2 - 5.58 \times 10^{-7} t^3$$

$$pK_{sp}^{AgI} = 17.874 - 7.85 \times 10^{-2} t + 2.65 \times 10^{-4} t^2$$

in the respective temperature ranges, 0−70 °C, 0−60 °C, and 10−40 °C.[14] The stability constants β_{11} at different temperatures are given from β_{11} at 25 °C in Table 1 and the enthalpy of formation of AgX monomers from Ag^+ and X^- ions, ΔH. According to refs 14 and 15, ΔH = -2.7 kcal mol^{-1} for AgCl and $\Delta H = -2.8$ kcal mol^{-1} for AgBr. However, since ΔH for AgI was unavailable in the literature, $\Delta H = -2.8$ kcal mol^{-1} for AgBr was assumed in the calculation for AgI. Theoretical γ^0 values of AgCl and AgBr bound by {100} faces and of spherical AgI at 10, 20, 25, 30, and 40 °C were calculated with these parameters. The results of the calculation are listed in Table 3 with the corresponding experimental results of γ. As is obvious from the experimental and theoretical γ values, there is an excellent agreement between them.

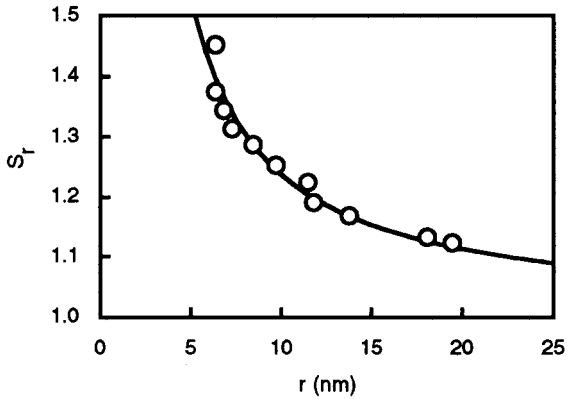

Figure 3. The relationship between the mean particle size and the supersaturation ratio of the standard AgCl dispersion at 25 °C and pCl = 3.0.

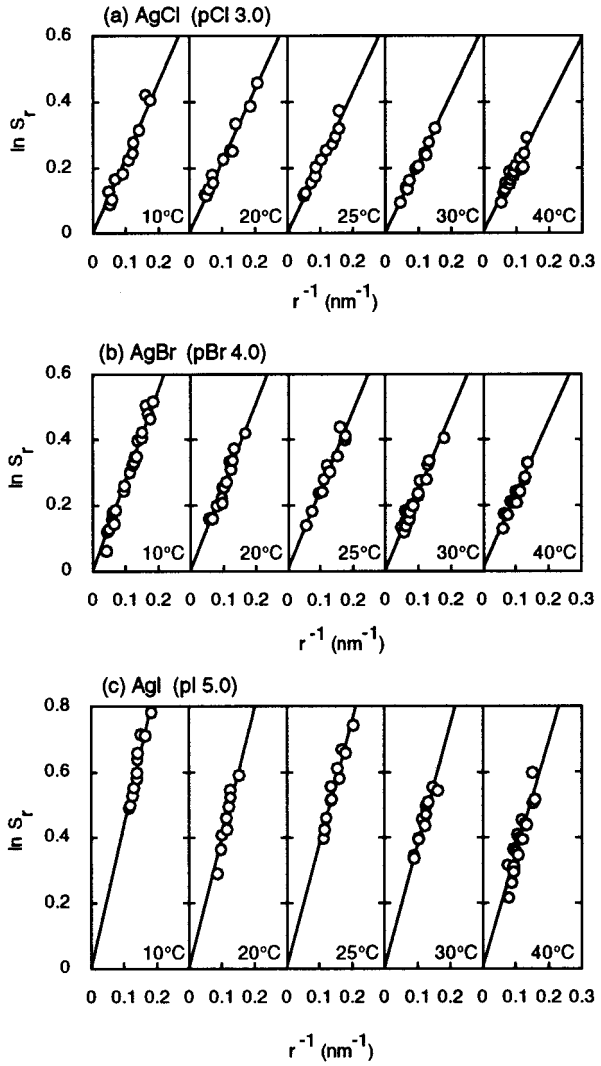

Figure 4. Correlations between ln S_r and r^{-1} based on the Gibbs−Thomson equation: (a) AgCl at pCl = 3.0; (b) AgBr at pBr = 4.0; (c) AgI at pI = 5.0.

6. Discussions

6.1. Assessment of the Present Theory. To date, the theoretical status of the solid−liquid interfacial energy remains far from satisfactory.

In relatively early theoretical studies, Benson and coworkers[17,18] tried to calculate the surface energy of alkali halides by taking into account the electrostatic, dipole−dipole, and dipole−quadrapole interactions and the Born repulsive forces among the surface ions. However, it does not seem that the theory based on the complex contributions of so many factors successfully describes the solid−liquid interfacial energy. Moreover, Walton[19,20] proposed a formula of γ_{hkl} for a $\{hkl\}$ crystal face, as a function of the lattice energy of the solid, the mean ionic radius, the structure factor proper to the $\{hkl\}$ face, and the number of ions in 1 mol of the solid. In this formula, however, the interactions between liquid and solid, as one of the decisive factors, are not taken into account. In addition, the disparities in the results among these theories are very large and we have no reasonable experimental data to support a particular one.

TABLE 3: Experimental γ and Theoretical γ ($=\gamma^0$) at Different Temperatures

	γ (mJ m^{-2})					
	AgCl		AgBr		AgI	
temperature (°C)	exptl	theor	exptl	theor	exptl	theor
10	104	102	112	111	128	125
20	102	101	107	109	120	122
25	102	101	104	109	116	121
30	102	101	105	108	117	119
40	100	100	102	107	112	116
facets		{100}		{100}		sphere

On the other hand, Turnbull[21] found a proportionality between the solid−melt interfacial energy and the heat of fusion for metals. Gránásy et al.[22] proposed a formula of γ for the solid−melt interfacial energy of metal for specific crystal faces taking the crystal surface structures into consideration on the basis of the proportionality between γ and the heat of fusion. This theory seems fairly reasonable if we consider that the heat of fusion may correspond to the difference in bonding energy between metal molecules in the melt and in the crystal. However, this result may not directly be applied to ionic crystal−solution systems. For example, although Kahlweit[23] found a proportionality between γ and the heat of dissolution for metal salts in the aqueous solutions, this finding may lack in theoretical bases, since the heat of dissolution involves the heat of dissolution involves the heat of dissociation of dissolved molecules and the heat of complexation, both of which are irrelevant to the interfacial energy.

As an approach from the solubility of a solid, Nielsen and Söhnel[24] proposed a formula of γ for metal salts in aqueous solutions on the basis of the solubilities of constituent ions. However, the extra interactions of ions, such as the electrostatic forces between individual cations and anions in a neutral molecule, dissociation of a molecule in the liquid phase, etc., involved in this treatment in addition to the indefinite concept of the ionic solubility have irrationalized the theory. Meanwhile, Mersmann[25] derived a formula for γ based on an integration of $d\gamma$ in the Gibbs adsorption equation for the increment of the concentration of the molecules as the constituent of the solid phase from the solubility level in the liquid phase to the concentration level in the solid phase. However, this treatment may need reconsideration, since $d\gamma$ in the Gibbs adsorption equation originally corresponds to the change of γ with the change of the equilibrium concentrations of nonmatrix components or foreign substances (see the Introduction of part 1[11]), and thus the integration of $d\gamma$ for the nonequilibrium concentration changes of the matrix components of the liquid and solid phases is not allowed. It may be readily understood if one considers that it is impossible to change the concentration of the solid component in the liquid phase from its solubility while maintaining the solid−liquid equilibrium at constant temperature

and pressure, and thus γ cannot be changed unless a foreign substance is added. Hence, what we can obtain from the Gibbs equation is only the change of γ by adsorption of foreign substances and not the absolute value of the original γ^0. In addition, even if we are apart from the original meaning of the Gibbs equation, the integration of dγ for the change of the chemical potentials of the solid and liquid components from the liquid phase to the solid phase across the interface involves a self-contradiction against the assumption of the uniform chemical potential of each component in this treatment according to the conventional rule.

The want of reasonable theory on the solid−liquid interfacial energy is no wonder in a sense, since fundamental studies based on the insight into the essential nature of the general interfacial energy itself have never been done until recently.

For the experimental determination of solid−liquid interfacial energy, although the number of reports is also rather limited, the methods may be classified into two main branches, i.e., kinetic methods based on the classical nucleation theories and thermodynamic methods based on the Gibbs−Thomson effect. For instance, Nielsen[3] obtained 100 mJ m^{-2} for AgCl, 200 mJ m^{-2} for AgBr, and 126 mJ m^{-2} for $BaSO_4$, while Sugimoto[7] reported 177 mJ m^{-2} for AgBr. These data were obtained by theoretical analysis on nucleation events. Meanwhile, 140 mJ m^{-2} for AgBr from potentiometry of silver ions with a certain size of AgBr particles by Berry,[8] 84 mJ m^{-2} for $SrSO_4$ from radiometry of ^{35}S in the supernatant liquid on natural sedimentation by Enüstün and Turkevich,[9] and 171 mJ m^{-2} for NaCl in absolute ethanol from conductometry of solubility with BET measurement of a ground NaCl powder by van Zeggeren and Benson[10] were based upon the Gibbs−Thomson effect.

Since the methods based on the classical nucleation theories are not free from many assumptions and approximations, high precision cannot be expected. In contrast, the simple Gibbs−Thomson equation is derived from the general thermodynamic principle without any assumptions and approximations. Hence, if the measurement of the size-dependent solubility is properly performed at equilibrium between the mean-sized particles and the solution phase, we can expect fully reliable results. However, the above measurements of γ based on the Gibbs−Thomson effect may be unsatisfactory on the criterion of properness in experimental conditions, since for accurate measurement we must satisfy several requirements, such as repeated solubility measurements with different particle sizes, rigorous in situ measurement of the solute concentration, and assessment of the effect of size distribution on the solubility as a whole. In this sense, the systematic potentiometry of solubility as a function of mean particle size from direct electron microscopy on instantaneous freezing, in the present study, may be in accord with these requirements.

Although the observed temperature dependence of γ^0 of these silver halides appears somewhat greater than the theoretical expectation, the small average deviations of the experimental γ^0 values from corresponding theoretical ones within a few percents (+0.49% for AgCl, −2.5% for AgBr, and −1.9% for AgI) seem satisfactory for the verification of the present theory as well as the Gibbs−Thomson effect, in view of the experimental errors and the allowances in the used thermodynamic parameters.

6.2. Shape Effects on γ and ψ_n^σ. If the shape factor of a particle having surface area A and volume V, $\boldsymbol{\beta}$, is defined by

$$\beta \equiv \frac{4A^3}{27V^2} \tag{6.1}$$

one obtains $\beta = 32$, $16\sqrt{2}$, and $16\sqrt{3}$for cube, dodecahedron, and octahedron, respectively. Since the surface area of a *n*-mer is represented by

$$A = \left(\frac{27\beta V^2}{4}\right)^{1/3} = \left(\frac{27\beta v_1{}^2 n^2}{4}\right)^{1/3} \tag{6.2}$$

the ratio of the surface areas per unit volume of a cube, dodecahedron, and octahedron is given by A_{cub}:A_{dod}:A_{oct} = 1:$(1/2)^{1/6}$:$(3/4)^{1/6}$ = 1:0.891:0.953. Since the intrinsic interfacial energy of an *n*-mer, $\psi^{0,\sigma}{}_n$, is given by

$$\psi_n^{0,\sigma} = \gamma^0 A \tag{6.3}$$

and since γ^0_{100}:γ^0_{110}:γ^0_{111} = 1:$\sqrt{2}$:$\sqrt{3}$ = 1:1.41:1.73, the ratio of intrinsic interfacial energies among these particles of the same volume is $\psi^{0,\sigma}_{n,cub}$:$\psi^{0,\sigma}_{n,dod}$:$\psi^{0,\sigma}_{n,oct}$ = 1:$2^{1/3}$:$(9/2)^{1/3}$ = 1:1.26:1.65. Hence, one may find that the total interfacial energy of a particle, $\psi_n^{0,\sigma}$, relative to its γ^0 can be lowered to some extent by reducing its specific surface area.

In particular, $\beta = 16\pi/3$ for spherical particles so that A_{cub}:A_{sph} = 1:0.806 and $\psi^{0,\sigma}_{n,cub}$:$\psi^{0,\sigma}_{n,sph}$ = 1:1.05. Since $\psi^{0,\sigma}_{n,sph}$ is higher than $\psi^{0,\sigma}_{n,cub}$ by only 5%, the stability of a sphere is rather close to a cube of the same volume, despite the great increase in γ^0 (γ^0_{100}:γ^0_{sph} = 1:1.30). This suggests that the reduction of the total surface area of a particle is quite effective in lowering its total surface energy, even if it causes the increase of the overall specific surface energy.

For cubic particles of the NaCl type, the {110} and {111} faces correspond to the surfaces of the edges and the corners, respectively. Even if the edges and the corners of the cube are truncated to form a higher polyhedron with a lower specific surface area, the total interfacial energy per unit volume may increase, as expected from $\psi^{0,\sigma}_{n,cub}$:$\psi^{0,\sigma}_{n,dod}$:$\psi^{0,\sigma}_{n,oct}$ = 1:1.26:1.65. Hence, a perfect cube is the most stable form for NaCl-type particles. However, if γ at the corners or edges of the cube is somewhat lowered by specific adsorption or other causes, it is possible to reduce the total interfacial energy below the level of the original cube of the same volume by rounding off or truncating the corners and edges, despite the increase of the overall γ. In this case, temperature dependence of γ must be enhanced due to the increase of $N^\sigma\lambda$.

Furthermore, in view of the easy formation of octahedral AgBr prepared at pBr <2.5,[26] the actual γ^0_{111} deems to be much lower than the theoretical γ^0_{111} = 188 mJ m^{-2}, since the difference between the theoretical γ^0_{111} and γ^0_{100} (=109 mJ m^{-2}) is too large to form the octahedral shape, even if we take into account that the growth form of microcrystals is not necessarily determined only by the energetic requirement,[26,27] to say nothing of the small effect of the halide adsorption on the reduction of γ, as will be shown in part 4. Since the shape of AgCl particles in the same fcc crystal system is always cubic under any preparation conditions unless some specific adsorptives are used,[28,29] it is likely that γ^0_{111} of AgBr is reduced by some electronic relaxation of the open sites of the {111} faces or depolarization between cationic and anionic sites, due to the greater covalent nature of AgBr than AgCl. If such a γ^0_{111}, considerably lowered but still significantly higher than γ^0_{100}, contributes to raising the overall γ^0 of AgBr particles, the greater temperature dependence of γ^0 is expected, as a sign of such an effect is observed in the experimental γ for AgBr in Table 3. Similarly, the spheroidal shape of AgI particles and their experimental γ values (=116 mJ m^{-2}), much higher than the

lowest γ^0 of β-AgI ($\gamma^0_{0001} = 89.4$ mJ m^{-2}), may also suggest the surface relaxation of the much higher γ values such as $\gamma^0_{10\bar{1}0}$ (=189 mJ m^{-2}) of β-AgI, γ^0_{100} (=156 mJ m^{-2}) of γ-AgI and γ^0_{111} (=180 mJ m^{-2}) of γ-AgI.

6.3. Solubility-Determining Particle Radius. In the present work, the mean radius of particles, $\bar{r}$, defined by

$$\bar{r} = \frac{\int_0^\infty f(r) r \, dr}{\int_0^\infty f(r) \, dr} \tag{6.4}$$

was employed as the effective size responsible for the solubility, where $f(r)$ is the size distribution function at radius r. In the experimental determination of γ on the basis of the Gibbs−Thomson effect, accurate determination of the mean equilibrium size is the most essential. Enüstün and Turkevich[9] suggested that the smallest particles determined the solubility in the $SrSO_4$/water system, since they found the best correlation between the Gibbs−Thomson equation and the smallest particle group in the size distribution, in addition to the fact that almost the same solubilities were obtained from systems containing the same minimum size group regardless of the average size. Such a situation may be observed when the rate of the Ostwald ripening is determined by the growth rate of the particles and not by the dissolution rate. Actually, it took as long as 2 months for the growth of $SrSO_4$ particles from 25 to 39 nm in average size in their system.

In contrast, the growth rate of silver halides is normally very fast. The growth of AgCl particles is usually controlled by diffusion of solute.[30] The growth of AgBr is also completely diffusion controlled in a certain range of bromide concentration ($2.6 \leq$ pBr ≤ 3.5),[26] and thus the growth mode of AgBr in our systems at pBr 4.0 close to this pBr range may be treated as diffusion-controlled growth. Moreover, the dissolution process of silver halides in general is thought to be diffusion controlled.[26,27] Therefore, it seems reasonable to use $\bar{r}$ in eq 6.4 as the equilibrium particle radius in the AgCl and AgBr systems, since the equilibrium particle radius in the diffusion-controlled Ostwald ripening is equal to the mean radius defined by eq 6.4, according to the theory of Wagner on Ostwald ripening.[31] On the other hand, the growth rate of AgI is normally very low due to the extremely small solubility. However, the ripening rates of AgI particles in our systems were found to be comparable to those of AgCl and AgBr particles, probably due to the exceedingly small size of the generated AgI particles, suggesting the applicability of eq 6.4 to the AgI systems as well.

6.4. Size Effect on Interfacial Energy. Tolman[13] discussed an effect of particle size on its specific interfacial energy on the basis of a liquid droplet−vapor system in equilibrium and proposed the following formula for the specific interfacial energy or surface tension as a function of the droplet radius r:

$$\gamma = \frac{\gamma_\infty}{1 + 2\delta/r} \tag{6.5}$$

where γ_∞ is the specific interfacial energy of the bulk liquid−vapor interface and δ is the distance from the Gibbs dividing surface (where the surface excess $\Gamma = 0$) to the surface of tension assumed to be located inside the Gibbs dividing surface of the droplet in the classical continuous interface model. Namely, he predicted that γ will decrease when a particle becomes extremely small. He considered the increase of chemical potential of the vapor, $d\mu$, by the Gibbs−Thomson effect and applied the Gibbs−Duhem relation to the droplet and vapor in equilibrium as

$$d\mu = \frac{dp_r}{\rho} = \frac{dp}{\rho'} \tag{6.6}$$

where p_r and p are the internal and external pressures of the droplet; ρ and ρ' are the number densities of the molecules in the liquid and vapor, respectively. Inserting this relation and the Laplace equation,

$$p_r - p = \frac{2\gamma}{r} \tag{6.7}$$

in the following basic equation like the Gibbs adsorption equation with Γ as the surface excess with respect to the surface of tension,

$$d\gamma = -\Gamma \, d\mu \tag{6.8}$$

he obtained

$$d\gamma = \frac{-\Gamma}{\rho - \rho'} d\left(\frac{2\gamma}{r}\right) \tag{6.9}$$

Finally, he derived eq 6.5 from this differential equation by formulating $\Gamma/(\rho - \rho')$ as a function of δ and r from integration of the density as a function of radial distance across the interfacial zone. However, one may find some fundamental problems in this theory as follows.

If one considers the formation of the droplet of radius r from a supersaturated vapor, the free energy of formation, ΔG, is given by

$$\Delta G = \frac{4}{3}\pi r^3 \rho(\mu_\infty - \mu) + 4\pi r^2 \gamma \tag{6.10}$$

where μ_∞ and μ are the chemical potentials of a molecule in the bulk liquid and in the supersaturated vapor, respectively ($\mu > \mu_\infty$). This formula reflects a sequential process of condensation of the supersaturated vapor to form bulk liquid of a volume equal to $4\pi r^3/3$ and subsequent formation of a droplet of the same volume in the vapor phase from the bulk liquid. If the droplet is in the equilibrium of vaporization and condensation with the supersaturated vapor, then $d(\Delta G)/dr = 0$ so that one obtains the following alternative expression of the Gibbs−Thomson equation on the assumption of γ being independent of r:

$$\rho(\mu - \mu_\infty) = \frac{2\gamma}{r} \tag{6.11}$$

Here, it must be noted that this equation can be derived only when γ is independent of droplet radius, and thus γ in eqs 6.10 and 6.11 must be equal to γ_∞ in eq 6.5.

Equation 6.11 clearly demonstrates that μ can be changed only by changing r without changing γ. On the other hand, eq 6.8 predicts that μ cannot be changed without changing γ. Hence, it is required to make clear the cause of this serious contradiction. Namely, if we ignore the minor effect of adsorption of vapor molecules, the chemical potential of an interfacial molecule of the droplet, μ^σ, can be approximated by μ^{σ_A} in the droplet-side surface layer ($\mu^\sigma \simeq \mu^{\sigma_A}$) and hence $d\gamma$ with the change of μ in the equilibrium system is given by

$$d\gamma = \Gamma(d\mu^{\sigma_A} - d\mu_r) \tag{6.12}$$

where μ_r is the chemical potential of an internal molecule in the droplet. If $d\mu^{\sigma_A} = 0$ and $\mu_r = \mu$, one may obtain eq 6.8. However, since the density and the change of pressure in the

σ_A layer are almost equal to those in the interior, $d\mu^{\sigma_A} \simeq d\mu_r$, and thus one obtains $d\gamma \simeq 0$ instead. Originally, the Gibbs adsorption equation, $d\gamma = -\sum\Gamma_i\, d\mu_i$, is valid only when $\sum\Gamma_i\, d\mu_i^{\sigma} \simeq 0$ at $dT = 0$ in a multicomponent system ($d\gamma = \sum\Gamma_i(d\mu_i^{\sigma} - d\mu_i) = -\sum\Gamma_i\, d\mu_i$). This condition in actually possible in the substitutional adsorption in a multicomponent system. In a single-component system, however, it is impossible to realize $d\mu^{\sigma_A} = 0$ and $d\mu_r \neq 0$ at the same time in eq 6.12, because the change of μ in a single-component system is always associated with the change of the internal pressure and thus the simultaneous change of μ^{σ_A} and μ_r. In short, the contradiction is due to the disregard of the pressure effect in the Gibbs adsorption equation.

It is now obvious that $d\mu^{\sigma} = 0$ was implicitly presumed in the theory of Tolman, and this is the reason why γ is lowered with increasing μ by reduction of particle size ($d\gamma = -\Gamma\, d\mu$), leading to eq 6.5. Hence, as the particle size is reduced to the level of a molecule, γ must be close to zero according to this theory. Such a situation is again unlikely, since even a vapor molecule liberated from the liquid phase by breaking the surrounding bondings must have open bonding sites of almost the same activity and surface density as those of the surface molecules of a vapor droplet.

As a consequence, there is no doubt that γ used in the Gibbs−Thomson equation (eq 4.1 or 6.11) is the size-independent γ_∞. This deductive conclusion is well in accord with our experimental results as well as those of Strey et al.[32] for droplets of 1-butanol in the vapor phase.

Incidentally, the surface tension or contractive force of the surface molecules of a droplet may not be kept constant when the size becomes so small as to have no internal molecules for strongly pulling the surface molecules. In such a size range, the surface tension is not equivalent to the specific interfacial energy anymore.

7. Conclusions

A new general formula of intrinsic specific interfacial energy of solid−liquid interfaces for spherical and polyhedral particles, $\gamma^0 = -N^{\sigma}\lambda kT \ln x_{(\infty)}$ in eq 2.12, has been derived from the fundamental theory of γ in ref 11 and collated to the experimental results of γ for silver halides determined by the Gibbs−Thomson effect. The excellent agreement for all kinds of silver halides of interest at different temperatures suggests the validity of the theoretical equation based on the fundamental theory.

Also, it has been shown theoretically and experimentally that γ is independent of particle size.

Appendix

Gibbs−Thomson Equation for Regular Polyhedral Particles. The free energy of formation of a particle consisting of n monomers (n-mer) from a supersaturated solution, ΔG, is represented by

$$\Delta G = -n\phi + \gamma A \tag{A-1}$$

where A is the surface area of the particle and

$$\phi \equiv \mu - \mu_\infty = kT \ln\frac{x}{x_{(\infty)}} \tag{A-2}$$

Here, μ and μ_∞ are the chemical potentials of a monomer in the supersaturated solution and in the bulk solid, respectively; x and $x_{(\infty)}$ are the mole fractions of the monomers in the supersaturated solution and in the solution in equilibrium with a bulk solid, respectively. If the particle is in the equilibrium of dissolution and deposition with the supersaturated solution,

$$\frac{d(\Delta G)}{dn} = -\phi + \gamma v_1 \frac{dA}{dV} = 0 \tag{A-3}$$

where v_1 and V are the volumes of a monomer and a n-mer, respectively. If the similarity of the shape is kept constant,

$$\frac{dA}{dV} = \frac{2A}{3V} \tag{A-4}$$

from $A \propto V^{2/3}$.

If the particle is a regular polyhedron with an inscribed sphere of radius r, V is related to A as

$$V = \frac{Ar}{3} \tag{A-5}$$

so that

$$\frac{dA}{dV} = \frac{2}{r} \tag{A-6}$$

Inserting eqs A-2 and A-6 in eq A-3, one obtains

$$x = x_{(\infty)} \exp\left(\frac{2v_1\gamma}{rkT}\right) \tag{A-7}$$

This is the general Gibbs−Thomson equation for regular polyhedral particles, in exactly the same form as eq 4.3 for a sphere.

References and Notes

(1) Becker, R.; Döring, W. *Ann. Phys.* **1935**, *5*, 719.
(2) Zeldovich, Y. B. *J. Exp. Theor. Phys. (Russ.)* **1942**, *12*, 525.
(3) Nielsen, A. E. *Kinetics of Precipitation*; Pergamon: New York, 1964; Chapter 4.
(4) Walton, A. G. *Mikrochim. Acta* **1963**, *3*, 422.
(5) Klein, D. H.; Smith, M. D.; Driy, J. A. *Talanta* **1967**, *14*, 937.
(6) Klein, D. H.; Smith, M. D. *Talanta* **1968**, *15*, 229.
(7) Sugimoto, T. *J. Colloid Interface Sci.* **1992**, *150*, 208.
(8) Berry, C. R. *Photogr. Sci. Eng.* **1976**, *20*, 1.
(9) Enüstün, B. V.; Turkevich, J. *J. Am. Chem. Soc.* **1960**, *82*, 4502.
(10) van Zeggeren, F.; Benson, G. C. *Can. J. Chem.* **1957**, *35*, 1150.
(11) Sugimoto, T. *J. Colloid Interface Sci.* **1996**, *181*, 259; **1996**, *183*, 299.
(12) Sugimoto, T. *J. Phys. Chem. B* **1999**, *103*, 3593.
(13) Tolman, R. C. *J. Chem. Phys.* **1949**, *17*, 333.
(14) Pouradier, J.; Pailliotet, A.; Berry, C. R. *The Theory of Photographic Process*, 4th ed.; James, T. H., Ed.; Macmillan: New York, 1977; Chapter 1.
(15) Sillén, L. G., Ed. *Stability Constants of Metal-Ion Complexes Section I*; Special Publication No. 17; The Chemical Society: London, 1964.
(16) Lewis, R. J., Rev. In *Hawley's Condensed Chemical Dictionary*, 12th ed.; Van Nostrand Reinhold: New York, 1993, p 1039.
(17) Benson, G. C.; Schreiber, H. P.; Patterson, D. *Can. J. Phys.* **1956**, *34*, 265.
(18) van Zeggeren, F.; Benson, G. C. *J. Chem. Phys.* **1957**, *26*, 1077.
(19) Walton, A. G. *J. Am. Ceram. Soc.* **1965**, *48*, 151.
(20) Walton, A. G. *The Formation and Properties of Precipitates*; Interscience: New York, 1967; Chapter 4.
(21) Turnbull, D. *J. Appl. Phys.* **1950**, *21*, 1022.
(22) Gránásy, L.; Tegze, M.; Ludwig, A. *Mater. Sci. Eng.* **1991**, *A133*, 577.
(23) Kahlweit, M. *Z. Phys. Chem. N. F.* **1961**, *28*, 245.
(24) Nielsen, A. E.; Söhmel, O. *J. Cryst. Growth* **1971**, *11*, 233.
(25) Mersmann, A. *J. Cryst. Growth* **1990**, *102*, 841.
(26) Sugimoto, T. *J. Colloid Interface Sci.* **1983**, *93*, 461.
(27) Sugimoto, T. *J. Colloid Interface Sci.* **1983**, *91*, 51.
(28) Claes, F. H.; Libeer, J.; Vanassche, W. *J. Photogr. Sci.* **1973**, *21*, 39.
(29) Leubner, I. H. *J. Imaging Sci.* **1985**, *29*, 219.
(30) Strong, R. W.; Wey, J. S. *Photogr. Sci. Eng.* **1979**, *23*, 344.
(31) Wagner, C. *Z. Elektrochem.* **1961**, *65*, 581.
(32) Strey, R.; Wagner, P. E.; Viisanen, Y. *J. Phys. Chem.* **1994**, *98*, 7748.